ELSEVIER

Materials Science and Engineering B80 (2001) 294–298

MATERIALS SCIENCE & ENGINEERING B

www.elsevier.com/locate/mseb

Proton-induced damage in p^+–n InP solar cells: the role of electron capture at high fluences

M.J. Romero [a,*], R.J. Walters [b], D. Araújo [a], S.R. Messenger [c], G.P. Summers [b], R.W. Hoffman, Jr [d,1], R. García [a]

[a] *Departamento de Ciencia de los Materiales e I.M. y Q.I., Facultad de Ciencias, Universidad de Cádiz, Apdo. 40, E-11510, Puerto Real, Cádiz, Spain*

[b] *Naval Research Laboratory, Code 6615, 4555 Overlook Avenue, S.W., Washington, DC 20375, USA*

[c] *SFA Inc., Largo, MD 20744, USA*

[d] *Essential Research Inc., Cleveland, OH 44122, USA*

Abstract

Through the technique of electron beam induced current (EBIC), the effects of proton irradiation on InP solar cells of p^+–n polarity have been investigated. InP cells of the opposite polarity (n^+–p) have been shown to collapse under heavy proton irradiation, due to carrier removal that first depletes and eventually type converts the base region. In contrast, we show that for cells of p^+–n polarity, electron capture plays the dominant role in the cell radiation response at high damage levels. © 2001 Elsevier Science B.V. All rights reserved.

Keywords: Proton irradiation; Solar cells; Electron beam induced current

PACS: 61.82.Fx; 84.60.Jt

1. Introduction

The service given by satellite-based, global communication systems is well known as used by most of us. The satellite networks currently under construction or in development are designed for Geosynchronous Earth Orbit (GEO) or Low Earth Orbit (LEO) (below $\sim$1600 km). GEO systems allow a global coverage with a minimum spacecraft, but they require high transmission power and may introduce long delay times. On the other hand, LEO systems allow a more rapid and a lower power transmission, but require a high number of spacecraft to attain a global coverage. The most advantageous orbits for a global satellite network, both from cost and operational viewpoints, may be in Medium Earth Orbits (MEO), in the 2000–10 000 km range [1]. Unfortunately, these orbits are in the midst of the Van Allen radiation belts, where the severe radiation environment causes a rapid degradation of the solar cells [2]. Among the few possible solutions for MEO satellite power generation, the InP-based technologies have been reported to be more radiation tolerant than current GaAs and silicon cells [3]. Very high efficiency InP cells of the n^+–p polarity show a collapse under heavy proton irradiation, caused by carrier removal that first depletes and eventually type converts the base region [4]. Therefore, we expect that higher radiation tolerance might be obtained if the polarity of the cell is inverted. This is an even more attractive prospect given the successful fabrication of high-quality p^+–n InP solar cells with efficiencies approaching 18% in Air-Mass Zero (AM0) [5]. In this paper, we report some results on the effect of proton irradiation on high-efficiency p^+–n InP cells by monitoring the electron beam induced current (EBIC) signal. This work is part of an ongoing collaboration between the University of Cádiz, Spain and the Naval Research Laboratory, USA to test the radiation tolerance of novel photovoltaic technologies.

* Corresponding author. Tel.: +34-956-016335; fax: +34-956-016288.

E-mail address: manueljesus.romero@uca.es (M.J. Romero).

[1] Present address: Ohio Aerospace Institute, Cleveland, OH 44135, USA.

PII: S0921-5107(00)00644-9

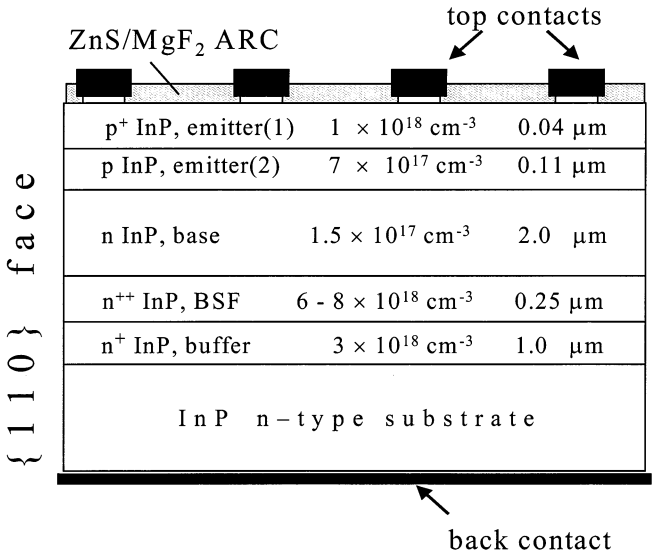

Fig. 1. Schematic diagram of the InP cells of p^+–n polarity.

2. Experimental details

The cells used here were fabricated by Essential Research, Inc (ERI) who have established the record of conversion efficiency for InP solar cells of p^+–n polarity (17.6%, AM0 1 Sun 25°C) [5]. The structure of the ERI cell is depicted in Fig. 1. For improving cell efficiency, instead of a uniform emitter, a p^+/p structure has been used to minimize defects related to Zn impurities. The cells were irradiated with 3 MeV protons up to a total fluence of 4.12×10^{14} cm^{-2} at the Pelletron Accelerator at the Naval Surface Warfare Center in White Oak, MD.

For EBIC measurements, the cells were mounted on an adapted holder of a JEOL-JSM820 scanning electron microscope. The induced signals were monitored both on {110} faces (perpendicular to epilayers) and at the cell surface, with the e-beam oriented along the [001] axis (Fig. 1). In this configuration, we measured the gain of the signal (the relationship between EBIC and e-beam current) at different acceleration voltages, between 6 and 30 kV. EBIC micrographs were also recorded from the {110} face. The interpretation of induced signals is assisted by simulations based on the finite element method (FEM).

3. Results and discussion

3.1. Analysis of the gain of the EBIC signal

EBIC measurements were made on several ERI cells that had been irradiated with 3 MeV protons up to fluences ranging from 10^{11} to 10^{14} cm^{-2}. Fig. 2 shows the electron beam energy dependencies of the EBIC gain for these cells. From the EBIC measurements, estimates of the base and emitter diffusion lengths were made for each cell. The results are detailed in Table 1. To evaluate the damage coefficient for this solar cell technology, the fluence is converted to displacement damage dose (D_d) by multiplying by the appropriate non-ionizing energy loss (NIEL) for protons in InP [6].

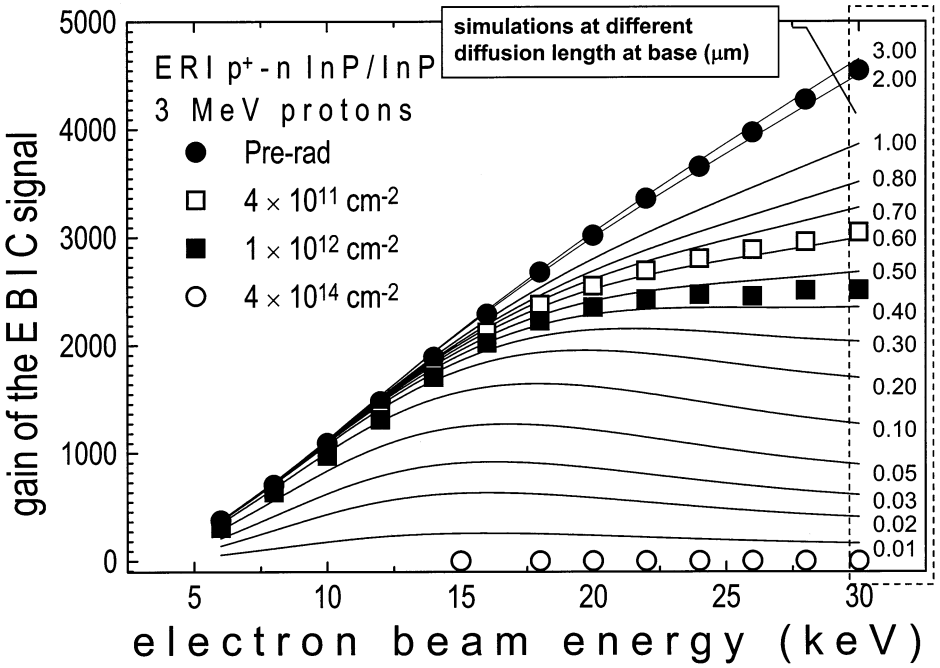

Fig. 2. Electron beam energy dependencies of the gain of the EBIC signal for proton irradiated cells with fluences ranging from 10^{11} to 10^{14} cm^{-2}. The gain has been simulated by the FEM method for different base diffusion lengths.

Table 1
Diffusion length in the base (n InP) and emitter (p InP), and surface recombination velocity (S/D, cm^{-1}) estimated from the analysis of the EBIC data for several proton irradiated ERI InP cells of p^+–n polarity

Fluence (3 MeV protons, cm^{-2})	Displacement damage dose (MeV g^{-1})	L_h (base) (μm)	L_e (emitter) (μm)	S/D (cm^{-1})
0	0	2.5 ± 0.2	0.17	10^5
4.16×10^{11}	8.45×10^9	0.62	0.10	10^4
1.04×10^{12}	2.10×10^{10}	0.45	0.10	10^4
4.12×10^{14}	8.37×10^{12}	–	–	–

A plot of the base diffusion length (L) versus D_d is shown as open squares in Fig. 3. Another estimate of L was made from spectral response (quantum efficiency) measurements for heavily proton-irradiated cells [7]. The data shown in Fig. 3 have been fit to the diffusion length degradation equation [8]:

$$\frac{1}{L(D_d)^2} = \frac{1}{L_0^2} + \kappa_L D_d \quad (1)$$

where L_0 is the pre-irradiation value of L and κ_L is the proton diffusion length damage coefficient. The fit gave a value for κ_L of 2.36×10^{-10} g cm^{-2} MeV^{-1}. This damage coefficient is comparable to $\kappa_L = 2.93 \times 10^{-10}$ g cm^{-2} MeV^{-1} determined for L in the p-type base of n^+–p InP cells [4].

The severe degradation of the gain at the highest levels of D_d ($> 10^{12}$ MeV g^{-1}) makes the analysis of the diffusion length difficult. The simulated data (Fig. 2) suggest that the diffusion length should have been degraded below 0.01 μm. However, even if diffusion processes were completely neglected (i.e. assuming $L =$ 0 μm), the simulation yields gain values above the experimental ones. This suggests that at higher fluences a second mechanism instead of diffusion length plays a main role in the degradation.

3.2. Monitoring the EBIC signal

Fig. 4 shows EBIC micrographs recorded from the {110} facets of two cells irradiated up to different proton fluences. The solid line is the average EBIC line-scan across the cell at each point, and the peak indicates the junction location. For cells irradiated up to a D_d of 2×10^{10} MeV g^{-1} and less, the signal level was reduced, but the location and shape of the peak was not affected. Based on this result, the radiation-induced damage in this fluence range can be described by degradation of the diffusion length.

After the D_d level exceed 8.4×10^{12} MeV g^{-1}, however, the irradiation caused a significant change in the signal peak, and the distribution began to spread and extend almost 1 μm into the base. This is consistent with a change in the cell spectral response observed at this fluence level, reported in Ref. [7]. In that report, it was thought that these effects were caused by carrier removal-induced changes in the cell structure, similar to those observed in heavily irradiated n^+–p InP cells. If this were true, then the carrier removal effects would have to be in the p-type emitter, because capacitance versus voltage (CV) measurements made on diodes of similar structure to the p^+–n InP cells show no radiation-induced change in the n-type base carrier concentration up to doses as high as 2×10^{11} MeV g^{-1} (Fig. 5). The cell structure would then be expected to have evolved from p^+–p–n to p–i–n, as the p-type emitter was driven intrinsic and the depletion region expanded into the emitter. However, the present EBIC results show that this is not the case.

As an alternative explanation, we now suggest that the observed junction degradation is a result of electron carrier capture at base. As shown previously [9], the primary radiation-induced defect in n-type InP is EB, which due to its energetic position, is an efficient electron trap. At high damage doses of 10^{11} MeV g^{-1}, these defects trap enough electrons to significantly reduce the free carrier concentration thereby increasing the bulk resistivity. This defect is electrically neutral after electron capture, so its presence does not affect the CV characteristic. Indeed, the EBIC measurements show a large increase in bulk resistivity at this damage level and the CV data (Fig. 5) show that the depletion region width was not affected.

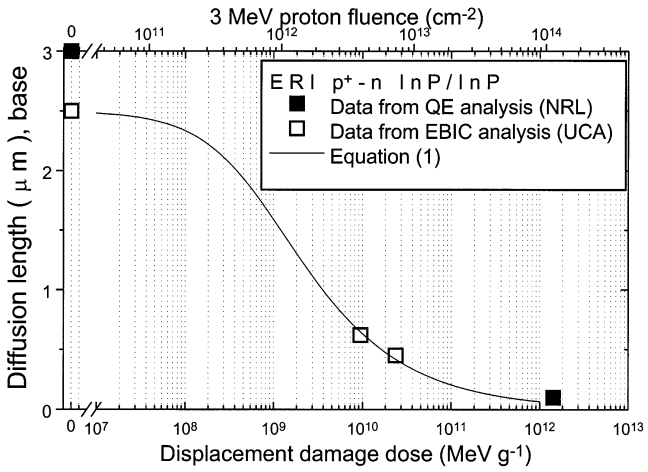

Fig. 3. A plot of the diffusion length in the base region of the ERI cells versus displacement damage dose, estimated from measurements of EBIC (at University of Cádiz) and spectral response (or QE, at Naval Research Laboratory). The curve is a fit of the data to Eq. (1).

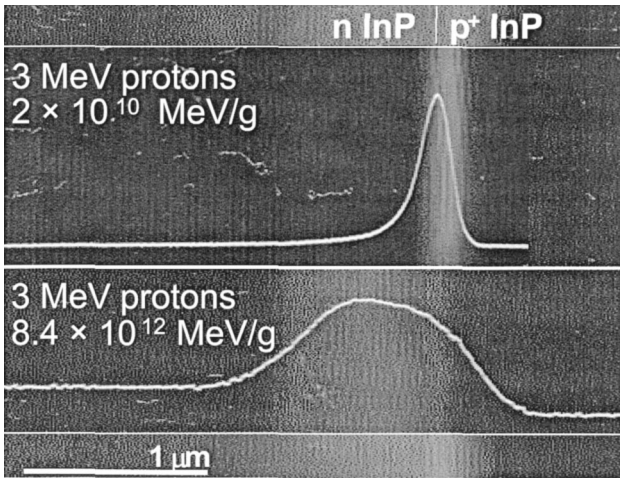

Fig. 4. EBIC micrographs from the {110} faces. The curve indicates the average EBIC line-scan throughout the cell. A significant change in the line-scan is apparent at high D_d levels. The micrographs were recorded with $E_b = 5$ keV and $I_b = 100$ pA.

Increasing the dose up to 10^{13} MeV g^{-1}, the EB density is comparable to the donor density at base and there are not enough free carriers for capture. EB keeps back its charge state. This midgap level changes the Fermi level and the depletion region width is extended, as shown by the EBIC measurements.

We have attempted to fit the measured EBIC line-scans by varying the diffusion length and electron carrier density in the various cell layers, and some of the results are shown in Fig. 6. For the cells irradiated up to D_d levels of 2×10^{10} MeV g^{-1} or less, good fits were obtained using the diffusion length estimates determined from the analysis of the EBIC gain (Eq. (1)).

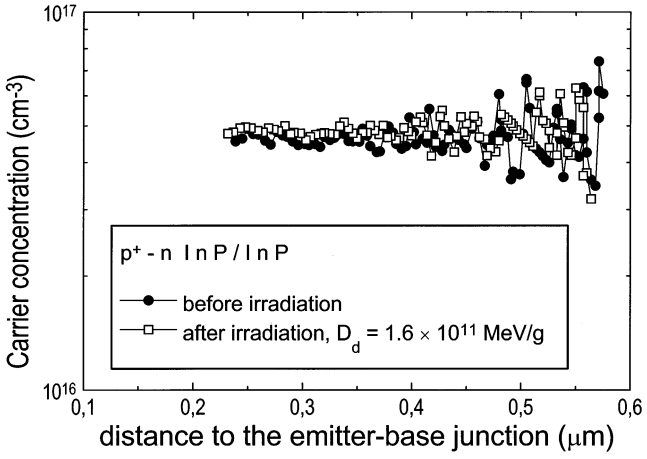

Fig. 5. Carrier concentration data determined from capacitance versus voltage measurements made on diodes of similar structure to the p^+–n InP solar cells before and after proton irradiation. The irradiation is seen to have no effect on the base carrier concentration at 10^{11} MeV g^{-1} of damage dose.

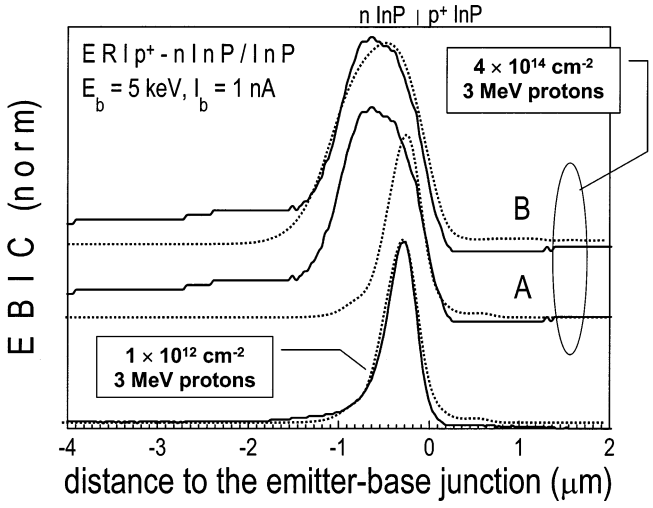

Fig. 6. Analysis of the EBIC line-scans measured on cells irradiated up to two different D_d levels. Experimental (solid lines) and calculated data (dotted lines) are shown. At the lower D_d level, the calculated data were obtained using a diffusion length value estimated from Eq. (1), and a good match to the experimental data is observed. At the higher D_d level, two calculated line-scans are shown, labeled A and B. Line-scan A was obtained assuming a diffusion length below 0.01 μm as suggested by Eq. (1). Line-scan B was calculated assuming a reduction of free carriers in $3–4 \times 10^{16}$ cm^{-3} throughout the n-type InP. Line-scan B clearly gives the best match to the experimental data.

Considering the higher D_d data, separate fitting attempts are shown in Fig. 6. The line-scan labeled A was calculated assuming a diffusion length less than 0.01 μm, and as expected from the results of Figs. 2–4, this yielded a poor fit to the experimental data. The best fit is obtained for line-scan B that was calculated assuming a EB density of $3–4 \times 10^{16}$ cm^{-3} throughout the n-type InP.

These results allow a qualitative analysis of the radiation degradation mechanisms in the p^+–n InP cells. At lower fluences, the primary damage appears to be degradation of the base minority-carrier-diffusion-length. At higher fluences, on the other hand, another damage mechanism appears to emerge, as diffusion length degradation alone is not sufficient to describe the measured data. In contrast to the case of n^+–p InP cells, this high-fluence damage mechanism does not appear to be a type conversion, but instead it may be attributed to electron capture by the primary radiation-induced defect EB in n-type InP, that is electrically neutral after capture. The free carrier concentration drops and the bulk resistivity shows a pronounced increase. Finally, when the EB concentration becomes comparable to donor density at base, the charge state of the defect is not screened and the junction shifts into the base.

4. Conclusions

The radiation-induced degradation of InP cells of p^+-n polarity has been analyzed through EBIC analysis. The results suggest that the primary degradation mechanism at high fluence levels is an increase in bulk resistivity due to electron capture by radiation-induced defects. Increasing the damage level even more, the electron capture exhausts and a spread of the depletion region is observed.

Acknowledgements

This work was supported in Spain by the CICYT (Comisión Interministerial de Ciencia y Tecnología) under MAT 94.0823.CO3.02 and by the Junta de Andalucía through group TEP-0120. The work at NRL was supported in part by Essential Research, Inc. through a Cooperative Research and Development Agreement (NCRADA-NRL-97-151) and by the U.S. Office of Naval Research.

References

[1] H. Keller, H. Salzwedel, G. Schorcht, V. Zerve, Proceedings of the IEEE 47th Vehicular Technology Conference. Technology in Motion (Cat. No. 97CH36003) (1997) 238.
[2] Semiconductor compound, 2(6) (1996), Compound Semiconductor Solar Cells for Satellite Communications.
[3] R.J. Walters, Microelectron. J. 26 (1995) 697.
[4] R.J. Walters, M.J. Romero, D. Araújo, R. García, S.R. Messenger, G.P. Summers, J. Appl. Phys. 86 (7) (1999) 3584.
[5] R.W. Hoffman, Jr., N.S. Fatemi, P.P. Jenkins, V.G. Weizer, M.A. Stan, S.A. Ringel, D.A. Scheiman, D.M. Wilt, D.J. Brinker, R.J. Walters, S.R. Messenger, IEEE 26th Photovoltaic Specialists Conference, Sept 30–Oct 3, 1997; Anaheim, CA.
[6] G.P. Summers, E.A. Burke, M.A. Xapsos, Radiat. Measure. 24 (1) (1995) 1.
[7] S.R. Messenger, R.J. Walters, G.P. Summers, R.W. Hoffman, Jr., Proceedings of the 2nd World Conference on Photovoltaic Energy Conversion, Vienna, Austria, July 1998, p. 3726.
[8] H.Y. Tada, J.R. Carter, B.E. Anspaugh, R.G. Downing, The Solar Cell Radiation Handbook, JPL Publications, 1982, p. 82.
[9] S.R. Messenger, R.J. Walters, M.J. Panunto, G.P. Summers, Proceedings of the 3rd Space Photovoltaic Research and Technology Conference, Cleveland, OH, 1994.